Sorption of Nitrogen Bases and XPS Study of Mesoporous Solid Acid SBA-15

Jeremy L. Smith, Richard G. Herman, Courtney R. Terenna, Matthew R. Galler, and Kamil Klier*

Department of Chemistry, 6 East Packer Avenue, Lehigh University, Bethlehem, Pennsylvania 18015-3102

Received: May 12, 2003; In Final Form: October 1, 2003

Mesoporous SBA-15 material (Melero, J. A.; Stucky, G. D.; van Grieken, R.; Morales, G. *J. Mater. Chem.* **2002**, *12*, 1664) contains a high concentration of $\equiv Si(CH_2)_3SO_3H$ functionalities accessible to ion exchange and adsorption of nitrogen bases. High-resolution XPS was used to determine stoichiometric equivalences between the $-SO_3^-$ groups and NH_4^+ cations exchanged for the $-SO_3H$ protons as well as between the $-SO_3H$ groups and adsorbed pyridine and ethylenediamine. XPS core-level shifts (CLS) of S2p photoemission to lower BEs identify the $-SO_3H$ groups as sites for cation exchange and donor hydrogen bonding to the adsorbed nitrogen bases. The N1s CLS to higher BEs identify the nitrogen atoms of pyridine and one of the two N atoms of ethylenediamine as acceptors of the hydrogen bond. The CLS are smaller than those previously observed in Nafion-H and sulfated zirconia (SZ) (Johansson, M.; Klier, K. *Topics Catal.* **1997**, *4*, 99). An all-electron, nonrelativistic DFT theory yields core-level orbital energies where shifts correlate well with the observed XPS CLS. As a result of this combined study, the propylsulfonic groups of the SBA-15 material are identified as weaker acids than those of Nafion-H and SZ, albeit ones with high surface concentration and excellent ion-exchange capacity.

1. Introduction

SBA-15 is a high surface area mesoporous thermostable solid acid with high proton concentration associated with propylsulfonic groups anchored on silica.[1,2] We prepared this material following the one-step synthesis of Margolese et al.[1] and reported the dehydrocondensation of alcohols to unsymmetrical ethers catalyzed by this material.[2] This reaction requires high surface concentration of Brønsted acid sites, since the mechanism is a dual site process, as indicated by kinetic analysis of the catalytic reaction on previously studied solid acids.[2−5] The hydrogen ion concentrations found were 1.2−2.2,[1,6] 1.6,[2] and presently 1.0 mequiv/g.

The mesoporous structure of SBA-15 is obtained by using an organic structure- directing agent that can subsequently be removed from the highly ordered two-dimensional siliceous mesostructure.

During the synthesis of SBA-15, mercaptopropyl groups are anchored onto the walls of the siliceous pores, and these groups are oxidized by H_2O_2 to form propylsulfonic acid moieties. In a previous synthesis of SBA-15, we showed by X-ray photoelectron spectroscopy (XPS) that only about 67% of the $\equiv Si(CH_2)_3SH$ groups were oxidized to $\equiv Si(CH_2)_3SO_3H$ species, but the material still contained an appreciable concentration of Brønsted acid sites.[2]

Goals of this research are to maximize the concentration of acid sites to facilitate the catalytic coupling of alcohols to form ethers and to determine the accessibility and strength of the acidic groups. Anchoring of dual acid sites in molecular proximity was previously achieved by molecular design of a "double pincer" bis(hydrogen sulfate) ethylene glycol precursor on zirconium hydroxide to yield a sulfated zirconia[7] that exhibited higher activity[3] than a traditionally prepared sulfated zirconia catalyst. With the SBA-15 catalyst, the degree of oxidation of propylthiol groups to sulfonic acid moieties as well as the proximity and strength of the acid groups need to be assessed to provide input into optimizing these materials for acid-catalyzed reactions.

We have employed high-resolution XPS to gain information in regard to the nature, strength, and concentration of acid sites on surfaces of solid catalysts. In particular, XPS can (a) identify the source of a proton donors and acceptors from core level shifts,[4,8] (b) distinguish between Brønsted acid and Lewis acid sites,[4,8] (c) provide a quantitative assessment of specific surface species involved in acid−base interactions,[4,7,8] and (d) distinguish between metal ions in cationic exchange sites and substitutional support framework locations.[9] The experimental results are supported and predicted by the theory of core levels, valence bands, and strength of base bonding to acid sites in optimized geometry.

In this paper, we report on the properties of the SBA-15 with respect to the adsorption of pyridine and ethylenediamine, representing nitrogen bases, and the exchange of the $-SO_3H$ protons with ammonium cations. The XPS analysis of experimental core-level shifts (CLS) is accompanied by the theory of relative orbital energies in the surface acid−base complexes and ion-exchanged sulfonic groups.

2. Experimental Methods

2.1. Synthesis. SBA-15 was synthesized by first dissolving 4 g of Pluronic 123 [poly(ethylene glycol)-*block*-poly(propylene glycol)-*block*-poly(ethylene glycol)], $EO_{20}PO_{70}EO_{20}$ (M_n = 5800, Aldrich) in 125 g of 1.9 M HCl. The mixture was then heated to 40 °C, at which point 32.8 mmol of tetraethoxysilane (TEOS) (99+% TEOS, Aldrich) was added. The mixture was then stirred and kept at 40 °C for 3 h during prehydrolysis. Next, 73.8 mmol of hydrogen peroxide (30% H_2O_2, Aldrich) and 8.2 mmol of 3-mercaptopropyltrimethoxysilane (MPTMS)

* Corresponding author. E-mail: kk04@lehigh.edu.

10.1021/jp0305990 CCC: $27.50
Published on Web 12/09/2003

(95% MPTMS, Aldrich) were added to the mixture, which was allowed to equilibrate at 40 °C for 20 h with stirring.

After this oxidation period, the mixture was transferred to a closed polypropylene bottle for aging and placed in a furnace at 100 °C for 24 h. The white solid that had precipitated was filtered, air-dried at room temperature, weighed, and subsequently refluxed in 95% ethanol for 24 h (400 mL of ethanol/1.5 g of dried material) to extract any remaining Pluronic. After the ethanol reflux, the material was filtered, washed sequentially with distilled water and absolute ethanol, and finally dried in an oven at 60 °C.

2.2. Characterization. High-resolution X-ray photoelectron spectroscopy (HR-XPS) was used to characterize the synthesized SBA-15. Electron microscopy (EM) was also used to determine the pore structure of SBA-15, the detailed description of which will be published elsewhere.[10] All XPS measurements were carried out using the Scienta ESCA-300 instrument at Lehigh University. Each sample was scanned initially with a brief survey from 0 to 1000 eV, followed by high-resolution scans of specific spectral regions including S2p, O1s, Si2p, C1s, and N1s orbitals. The 2p spectral regions of metals whose ions were used in the ion-exchanged SBA-15 samples were also scanned.

The Scienta ESCA-300 instrument combines a high-power rotating anode X-ray source with monochromatization (Al Kα) and 300-mm mean radius hemispherical electron energy analyzer (HMA) to offer high sensitivity and resolution at acceptable scan times.[8,11,12] Because SBA-15 is an insulating sample, a hot filament flood gun provides low energy electrons (0−10 eV) during analysis to minimize positive charge buildup on the sample surface.[11] All samples were pressed in open atmosphere onto double-sided sticky tape, forming a wafer. Based on estimates made by Hunsicker et al., XPS analysis of very porous materials provides a bulk analysis because of the large escape depths.[9]

Quantitative analysis was performed using the ESCA analysis software from Scienta. After integration, peak areas were converted to corresponding concentrations by dividing them by their respective "sensitivity factors." These factors are instrument specific, and they are effectively response factors specific to each orbital of each element, referenced to the sensitivity factor for the 1s orbital of carbon (C1s) being 1.0000. The sensitivity factors used herein were 1.630 for N1s and 1.679 for $S2p_{3/2}$ and $S2p_{1/2}$ combined.

To determine the relative binding energies (BEs) of insulating samples,[13a] a useful method is to reference the measured BE to an internal or external standard, thereby allowing the comparison of spectra. Here, all BE values are referenced to the Si2p BE being 103.5 eV. All BE values at peak maxima were obtained from fast Fourier transform (FFT) filter smoothing of the data.

In addition to the ESCA analysis, the multipoint Brunauer, Emmett, and Teller (BET) method[14] was used to measure the total surface area of the synthesized SBA-15, employing a Gemini 2360 V1.03 instrument for the procedure. A series of measurements was made wherein a given mass of sample was heated to 120 °C for 1−2 h under nitrogen gas flow, subsequently re-weighed, and the surface area redetermined. This procedure was repeated until there was no change in the mass of the sample, nor in the BET surface area. To determine its acid exchange capacity, a 50-mg portion of the SBA-15 material was dispersed into 10 g of 2 M $NaCl_{(aq)}$, to which phenolphthalein was added as an indicator. The mixture was then titrated with 0.1 M $NaOH_{(aq)}$. From the volume of titrant solution, the acid exchange capacity was determined in units of mequiv of H^+/g of material.

X-ray powder diffraction (XRD) was used to determine the pore size of the SBA-15 from the observed diffraction pattern using the low angle 2θ peak. XRD data was collected on a Siemens D5000 instrument in parallel beam geometry with CuKα radiation and a $\theta-\theta$ goniometer. X-ray optics included a Göbel mirror on the incident beam side with Soller slits and a LiF monochromator on the diffracted beam side. The diffraction pattern was utilized to assign the reflections of particular atomic planes that match a hexagonal lattice and to determine the unit cell dimension.

2.3. Nitrogen Base Adsorption and Ammonium Exchange. The synthesized SBA-15 material was used in both the adsorption of nitrogen bases from hydrocarbon solution and ammonium exchange from 0.1 M aqueous solution of ammonium chloride (10 mL of $NH_4Cl_{(aq)}$ over 0.1 g of SBA-15 for 1 h at 298 K, filtered, washed with distilled water, and dried at 115 °C).

Adsorption of the nitrogen bases was carried out in refluxing solutions. After refluxing 300 mg of SBA-15 for 4 h in a solution of 0.03 mL of ethylenediamine (En) in 100 mL of cyclohexane, with a 50% molar excess of En, the reaction mixture was cooled and filtered using Whatman No. 2 filter paper under a vacuum provided by an aspirator. The solid was washed several times with cyclohexane to ensure that all excess, unbound En was removed from the SBA-15 material. The mostly dry solid was then placed in a 110 °C oven for 10 min. The same procedure was also used to titrate the SBA-15 with the nitrogen base pyridine (Py) by refluxing 200 mg of SBA-15 for 4 h in a solution of 0.03 mL of anhydrous pyridine (Aldrich, 99.8%) in 100 mL of cyclohexane, again with a 50% molar excess of Py.

The XPS analysis of the N1s region of the nitrogen base and the S2p region of the sulfonic groups of the SBA sorbent included quantitative assay of the elements and CLS. The C1s analysis is also reported for total carbon assay and, together with Si2p, for referencing of the CL energies.

3. Theoretical Methods

The models adopted to represent the single and dual propylsulfonic acid sites anchored on the silica wall of the SBA-15 material are specified by the chemical formulas

$$\mathrm{HS\text{-}CH_2{\cdot}CH_2{\cdot}CH_2\text{-}Si(H_2)\text{-}O\text{-}Si(H_2)\text{-}CH_2{\cdot}CH_2{\cdot}CH_2\text{-}}\boldsymbol{SO_3H}$$

"single site" (I)

and

$$\boldsymbol{HO_3S}\text{-}\mathrm{CH_2{\cdot}CH_2{\cdot}CH_2\text{-}Si(H_2)\text{-}O\text{-}Si(H_2)\text{-}CH_2{\cdot}CH_2{\cdot}CH_2\text{-}}\boldsymbol{SO_3H}$$

"dual site" (II)

The highlighted $-SO_3H$ groups are the active sites and the $-SH$ groups are inert to both ion exchange and nitrogen base adsorption, as shown by all calculations. The $-SO_3H$ groups are hydrogen donors for bonding with neighboring sulfonic groups, with nitrogen bases, and are proton-exchange and cation-exchange sites. When there is a hydrogen-donating group in the vicinity, the lone electron pairs of doubly bonded oxygen atom of the O═S(O)OH group will act as a hydrogen bond acceptor. To simulate the rigidity of the silica wall, the seven atoms of the −Si−O−Si− backbone capped by four hydrogen atoms were kept frozen in all geometry optimizations in which all other atoms in the bare sites I and II, as well as their complexes with neutral molecules or ions, were allowed to move.

The density functional theoretical (DFT) calculations[15] were performed at an all-electron, generalized gradient approximation (GGA) at a nonrelativistic level using the Becke−Perdew functional[16,17] and the double-numerical basis set of Delley,[18] similarly as in our earlier work on models of acid sites in fluorocarbon sulfonic acids, sulfated zirconia (SZ), tungstena-zirconia (WZ), and transition states for dehydrocondensation of alcohols to ethers.[4,19,20] These calculations yield total energies of the reactants, sorption bonding energies, and optimized geometries. In addition, the calculated orbital Kohn−Sham (KS) energies afford a comparison of chemical CLS with those observed in XPS. Because of the presently employed nonrelativistic level of calculation, the core-level spin−orbit split states $S2p_{3/2}$ and $S2p_{1/2}$ are represented by the KS energies disregarding the spin−orbit interactions, i.e., as S2p. This approximation is sufficient for the correlations revealed in this work because the experimental XPS 2p levels are incompletely resolved. On the contrary, the N1s and C1s levels are not spin−orbit split in experiment or theory. The final state energies involving core−hole states have not been calculated, assuming that, although the final states contribute to absolute photoemission energies quite significantly, they will have little influence on relative positions of the core levels between similar molecular species in the presently studied closed-shell molecules.[21]

That the present theoretical approach is sufficient for interpretation and prediction of CLS is supported by the agreement between the previously observed experimental difference of the S2p CLS in the −SH and $-SO_3H$ moieties, reported as 5.15 eV,[2] and the presently calculated difference between the corresponding KS S2p orbitals, 5.27 eV. In addition, the present theory correctly accounts for the simultaneous shift of N1s core levels of the nitrogen bases to higher BEs and S2p levels of the $-SO_3H$ groups to lower BEs upon the formation of the $-SO_3H\cdots$nitrogen base complex.[8] Higher level, fully relativistic calculations involving both the initial and the final states are feasible and appear necessary for the interpretation of CLS in *metal alloys*,[22] and have also been employed in the theory of CLS which establishes the correlational relationship between the total energies and the KS orbital energies in zeolites.[21] However, the present correlation between theoretical orbital energies and experimental BEs indicates that the relative core-level chemical shifts in *insulators* are qualitatively and semi-quantitatively accounted for by the initial KS orbital energies.

4. Results

4.1. Experimental Results. The synthetic route employed in the present work gave rise to mesoporous silica SBA-15. The BET surface area was found to be 551 m^2/g, and the sodium hydroxide titration of the material gave an acid exchange capacity of 1.00 mequiv of H^+/g. XRD analysis yields a well-resolved pattern of one prominent peak at a small 2θ value and two weak peaks at slightly larger 2θ values. The peaks can be indexed to a hexagonal lattice, where the d spacings correspond to a large hexagonal unit cell dimension and hexagonal close-packed parallel pores.[1,2,6,23−26] The XRD pattern here gave a hexagonal unit cell dimension ($a_0 = 2d(100)/\sqrt{3}$) of 14.5 nm with spacings $d(100) = 12.6$ nm, $d(110) = 7.3$ nm, and $d(200) = 6.3$ nm. Knowing the proton concentration of 1.00 mequiv/g, the surface area of 551 m^2/g, and having calculated the silicon surface concentration to be 8.22 Si atom/nm^2 previously,[27] one can calculate the molar equivalence of protons per silicon atom. This value is found to be 0.133, equivalent to 7.52 Si atoms per proton.

HR-XPS analysis of each sample was carried out and each spectrum was shifted to the reference BE of Si2p = 103.5 eV.

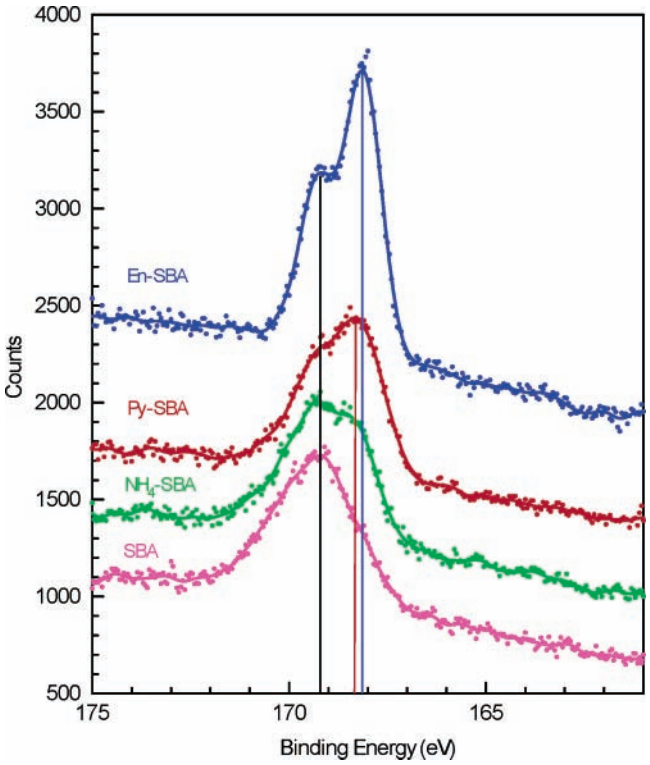

Figure 1. S2p regions of SBA-15 material with adsorbed nitrogen bases. Data are color coded and stacked additively. FFT filter smoothed line plots are shown with data points.

XPS of the material showed a single S2p peak at 169.25 eV with a full width at half-maximum (fwhm) of 2.63 eV and a C1s peak at 285.00 eV with a fwhm of 2.43 eV. Dividing the C1s concentration percentage by that of the S2p gave a carbon-to-sulfur ratio (C/S) of 2.9. Figures 1 and 2 show the S2p and C1s regions of the pure SBA-15, respectively.

XPS results from the adsorbed nitrogen bases are summarized in Table 1. For the *ethylenediamine adsorbed on SBA-15 (En-SBA)*, two N1s peaks of equal intensity separated by 2.05 eV were observed. There is only one S2p peak, at 168.15 eV, with a fwhm of 2.01 eV. The ratio of areas of the S2p and N1s peaks (i.e., the area of both nitrogen peaks combined) is 1.0. The C1s peak was observed at 285.15 eV and has a large shoulder to higher BEs, at approximately 286.45 eV. The fwhm of the C1s peak is 2.56 eV.

The *pyridine adsorbed on SBA-15 (Py-SBA)* was found to have a S/N ratio of 2.5, with only one N1s peak observed. The N1s peak is at 402.15 eV, and it has fwhm of 1.87 eV, with a slight tail to the lower BE side. The S2p peak for the py-SBA has a BE of 168.45 eV and a fwhm of 2.41 eV. The C1s peak was found to be at 285.25 eV, with a fwhm of 2.46 eV. The S2p, C1s, and N1s regions of the SBA-15 material after the sorption of nitrogen bases are shown in Figures 1, 2, and 3, respectively.

The *ammonium-exchanged (NH_4-SBA)* material yielded S/N = 3.5, C/N = 8.95 and C/S = 2.55, respectively. The single N1s peak has a BE of 402.60 eV with fwhm of 2.45. The maximum of the S2p peak is at 169.30 eV, but there is a second, overlapping peak on the lower BE side at 168.60 eV with fwhm of 2.85 eV entailing both S2p peaks. The C1s is at 285.20 eV with fwhm of 1.84 eV.

4.2. Theoretical Results. 4.2.1. Models for SBA. The optimized geometries of the bare single-site (I) and dual-site (II) assemblies shown in Figure 4 reveal a significant hydrogen donor−acceptor bonding between the neighboring $-SO_3H$

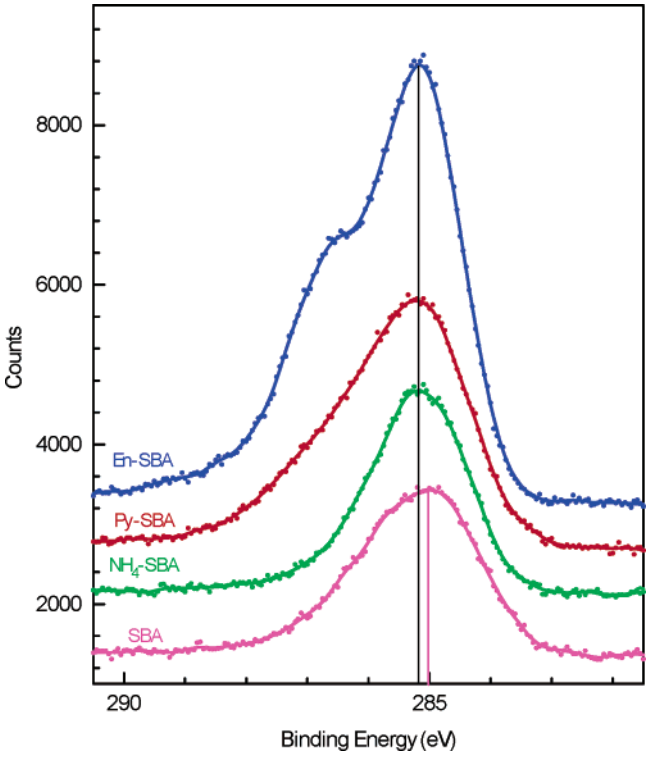

Figure 2. C1s regions of SBA-15 material with adsorbed nitrogen bases. Data are color coded and stacked additively. FFT filter smoothed line plots are shown with data points. The main peak of En-SBA is emission from the propyl-sulfonic groups, and the shoulder at higher BE is from the carbons of ethylenediamine.

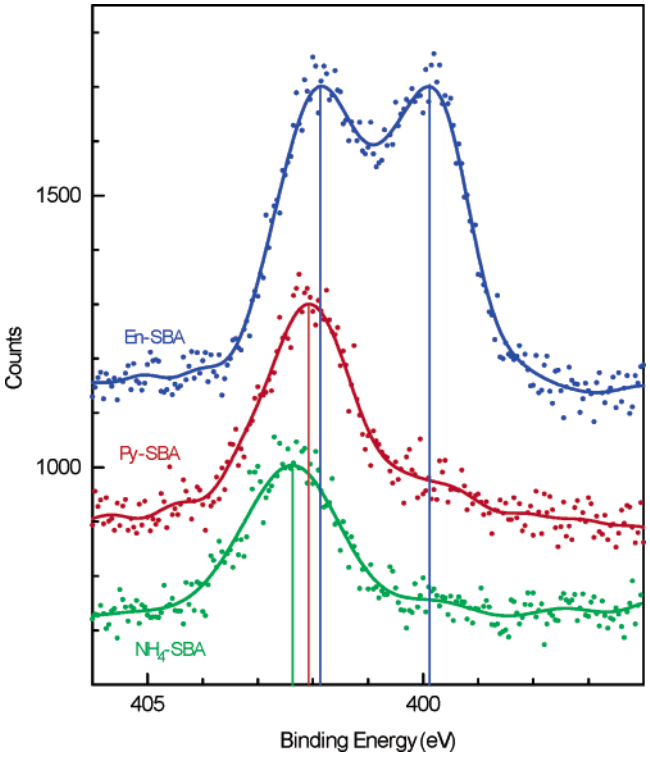

Figure 3. N1s regions of SBA-15 material with adsorbed nitrogen bases. Data are color coded and stacked additively. FFT filter smoothed line plots are shown with data points.

TABLE 1: Stoichiometric Equivalences, Binding Energies,[a] Peak Widths, and Chemical Shifts for the SBA-15 Material with Adsorbed Nitrogen Bases

Species	S/N Ratio	S2p BE(eV)	S2p fwhm(eV)	N1s BE(eV)	N1s fwhm(eV)	ΔBE (eV)[b]
En-SBA	1.0	168.15	2.01	399.80	-	231.65
				401.85	-	233.70
Py-SBA	2.5	168.45	2.41	402.15	1.87	233.70
NH_4-SBA	3.5	169.30	2.85	402.60	2.45	233.30
		168.60				234.00
SBA	-	169.25	2.63	-	-	-

[a] All BEs referenced to Si2p = 103.5 eV. [b] This is the separation of the N1s peak from the S2p peak for the given sample, i.e., N1s − S2p.

groups of the proximal sites (II), while such a hydrogen bonding is absent in the single-site moiety (I).

The complexes with adsorbed En, Py, and ammonia shown in Figure 5 reveal a stronger hydrogen bond between the $-SO_3H$ group and the nitrogen base in which, however, the proton of the sulfonic group is not completely transferred to the nitrogen to form an "ammonium ion". The sorption energies of the three nitrogen bases were calculated for both the single sites depicted in Figure 5 and the dual sites, as summarized in Table 2. The adsorption energy on dual sites is substantially smaller than that on the single sites due to repulsive interactions between the adsorbates in molecular proximity.

The calculated KS orbital energies for the various complexes studied on sites I and II are summarized in Table 3 and Figure 6. For the sake of comparison with experiment in section 4.1, only the S2p and N1s orbital energies are listed, although of course all the core and valence levels have been calculated.

4.2.2. Models for Hydrocarbon− vs Fluorocarbon−Sulfonic Acids. Models in which the alkyl chain carrying the $-SO_3H$ functionality is modified by halogen substitution are useful for understanding, control and design of acid catalysts. Substitution of fluorine for hydrogen in the alkyl-sulfonic group affects the acid strength of the $-SO_3H$ goups as well as the XPS CLS, as exemplified by calculations summarized in Table 4.

The sorption energies and CLS are accompanied by a pronounced proton shift from the $-SO_3H$ group to the nitrogen base induced by the presence of the backbone fluorine, as shown in Figure 7.

4.2.3. General Pattern of Nitrogen CLS−A Comparison with Experiment. Nitrogen CLS have been used for characterization of organic compounds with heterocyclic, amine, amide, nitrile, and nitro organic compounds. The application of XPS to the diagnostics of solid acid−base interactions is reinforced by a theoretical treatment, at the present level, of a large database of organic polymeric materials accumulated by Beamson and Briggs.[13b] Correlation between experiment and theory of reference compounds justifies the extension of the theory into a predictive realm of subtle effects of molecular environment and weak interactions examined in the previous sections. We therefore provide such a correlation using the calculated *orbital energies* rather than those previously employing effective atomic charges calculated by semiempirical methods,[8,28] later refined for polarizabilities and other molecular parameters of conjugated π-systems[29] which, however, did not produce satisfactory or predictive results.[8] Even though the Beamson−Briggs database entails polymers, it is evident from the data that segments and pendant groups can be modeled by capped molecular units.

The results based on a comparison of the calculated orbital energies and XPS binding energies are presented in detail in the Supporting Information section, and are summarized herein as follows:

(a) The experimental N1s BEs of the 22 nitrogen-containing polymers listed in the Beamson−Briggs database span a range of ∼10 eV and are given with a precision to 0.01 eV.

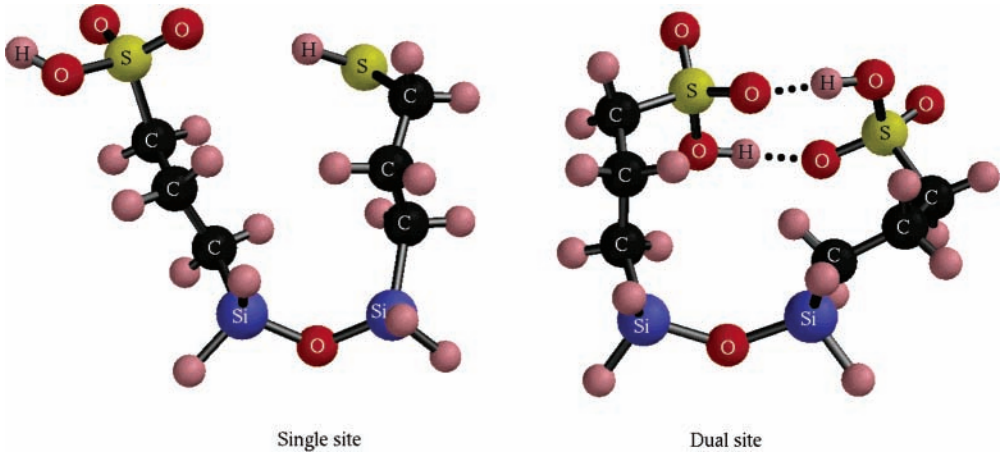

Figure 4. Models for the propylsulfonic pendant groups in the SBA material: single site (formula I) and dual site (formula II). The thiol group in the single site is inert and the distance −SH···O═S is 0.25 nm. The dotted lines in the dual site mark a weak double hydrogen bonding with distances OH···O═S equal to 0.16 nm.

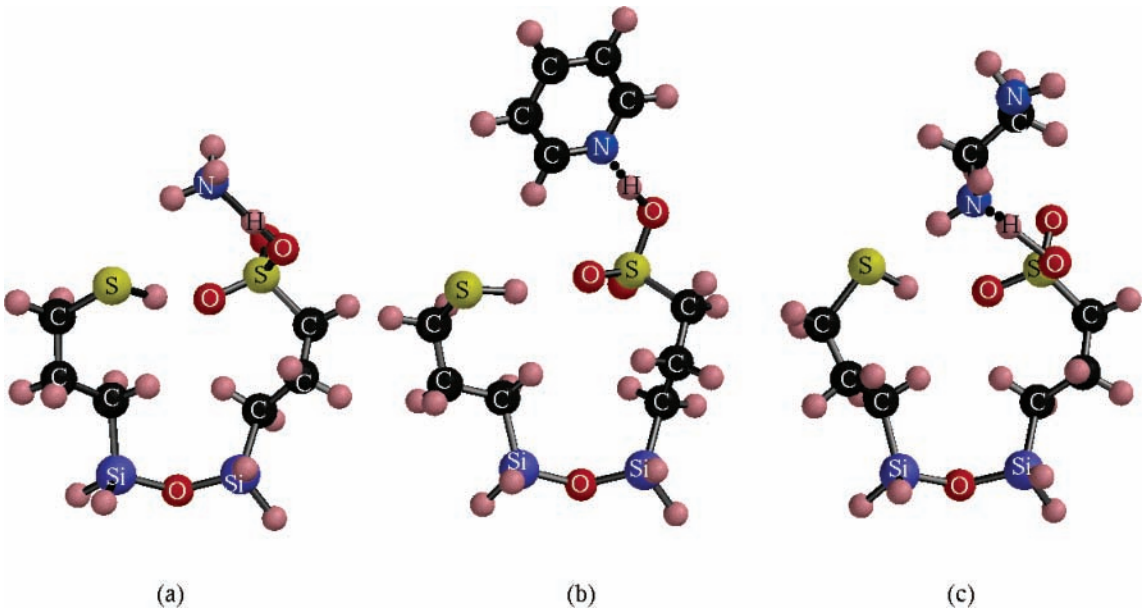

Figure 5. Single site complexes with nitrogen bases: (a) ammonia, (b) pyridine, (c) ethylenediamine. The hydrogen bonding distances $-O_2SO\cdots H\cdots N$ are, in nm, (a) 0.108 (O···H) and 0.152 (H···N), (b) 0.110 (O···H) and 0.148 (H···N), and (c) 0.153 (O···H) and 0.111 (H···N). All the −SH groups are inert to the nitrogen base adsorption and far enough from the SO_3H sites, 0.21−0.22 nm, indicating an extremely weak, if any, hydrogen bonding $-SH\cdots O{=}SO_2H$.

TABLE 2: Adsorption Energies of Nitrogen Bases on Propylsulfonic Acid Sites. Energies Are Given in kJ/Mol of Adsorbate

adsorbed molecule	NH_3	pyridine	ethylene diamine	ethylene diamine on bridging sites
single site[a]	−75.3	−54.4	-96.2	
dual site[b]	−46.0	−33.5	-33.5	-83.7

[a] $M\cdots HO_3S(CH_2)_3-Si-O-Si-(CH_2)_3SH$. M is the adsorbed molecule. Si atoms are capped by 2 H atoms each. [b] $M\cdots HO_3S(CH_2)_3-Si-O-Si-(CH_2)_3SO_3H$...M. When M is ethylenediamine (En), column 4 shows adsorption energy per En with each $-SO_3H$ bonding one En molecule, and column 5 shows adsorption energy per En with one En molecule bridging the two $-SO_3H$ sites.

(b) The calculated orbital energies E(N1s) in the nitrogen-containing segments defined in Table S1, rounded off to 0.01 eV, span the same range and correlate linearly with the experimental data as $[-E(\text{N1s}) = (0.999 \pm 0.0003) \times \text{BE-(N1s)}_{\text{corr.}} - 18.20]$ eV (Table S2 and Figure S1).

(c) Experimental reference levels for aliphatic carbon BE-(C1s) = 285.0 eV[13b] were refined based on calculations of C1s orbital energies which yield somewhat different values for different polymer segments. This procedure yielded adjusted $\text{BE(N1s)}_{\text{corr}}$ as defined and listed in Table S2 and used in the correlation (b) above.

As a result, the correlation between the calculated N1s orbital energies and experimental BEs provides a strong support for the use of XPS in conjunction with theory for a quantitative assessment of energies and structural changes resulting from interactions with molecular environment, including weak hydrogen bonding.

5. Discussion

The pendant propyl-sulfonic groups of the SBA material are identified as hydrogen-donor sites in the $-(CH_2)_3SO_3H\cdots N-$ base sorption complexes by the S2p and N1s core-level shifts in opposite directions. The precursor mercaptopropyl groups, which are present in incompletely oxidized SBA, are inert.

TABLE 3: Kohn−Sham Orbital Energies of Propylsulfonic Acid Sites with Nitrogen Bases (All Energies in eV)

site[a]	BE(S2p)	BE(N1s)	Δ(S2p)	Δ(N1s)
SingleSite.S1	−160.10		0.00	
SingleSite.S2	−154.83		5.27	
DualSite.S2	−160.29		−0.19	
SingleSite.En.S1	−158.31	−383.19	1.79	−2.72
SingleSite.En.S2	−154.87	−381.64	5.23	−1.17
DualSite.En.S1	−159.78	−382.76	0.32	−2.29
DualSite.En.S2	−158.97	−382.07	1.13	−1.60
SingleSite.Py.S1	−159.25	−382.48	0.85	−2.01
SingleSite.Py.S2	−154.60		5.50	
DualSite.Py.S1	−159.32	−382.80	0.78	−2.33
DualSite.Py.S2	−159.47		0.63	
DualSite.2En.S1.N1	−159.02	−382.92	1.08	−2.45
DualSite.2En.S1.N2	−159.02	−381.46	1.08	−0.99
DualSite.2En.S2.N1	−159.61	−382.24	0.49	−1.77
DualSite.2En.S2.N2	−159.61	−380.62	0.49	−0.15
SingleSite.NH3.S1	−159.37	−382.11	0.73	−1.64
SingleSite.NH3.S2	−154.87		5.23	
DualSite.2NH3.S1	−159.60	−382.46	0.50	−1.99
DualSite.2NH3.S2	−158.53	−381.96	1.57	−1.49
NH3		−380.47		0.00
En.N1		−380.57		−0.10
En.N2		−380.52		−0.05
Py		−381.03		−0.56

[a] The single site is modeled as $HO_3S(CH_2)_3-Si-O-Si-(CH_2)_3SH$. The sulfur of the sulfonic group is denoted S1 and that in the thiol group as S2. Each S2p level BE(S2p) is averaged over the $2p_x$, $2p_y$, and $2p_z$ orbitals. The dual site is modeled as $HO_3S(CH_2)_3-Si-O-Si-(CH_2)_3SO_3H$, and the two sulfur atoms, S1 and S2, have S2p average levels as above. The spread of the 2p orbitals due to their structural nonequivalence is shown in Figure 6. The Si atoms are capped by two H atoms each. The adsorbed molecules, whose N1s orbital energies are given as BE(N1s), are ethylenediamine (En) with two nonequivalent nitrogens, pyridine (Py), and ammonia (NH_3). Single and dual sites exchanged with the NH_4^+ ions are obtained by replacing the protons of one or two $-SO_3H$ groups. Adsorbed ammonia is equivalent to $-SO_3NH_4$. The orbital energy chemical shifts for the "bare sites" (rows 1−3), adsorbed complexes (rows 4−15), and ion-exchanged species (rows 16−19) are represented as Δ(S2p) referenced to the average S2p energy of the $-SO_3H$ group in the single-site model (row 1, column 4) and Δ(N1s) referenced to the N1s energy in free ammonia (row 20, column 5). The levels of calculation and geometry optimization are described in text.

Ethylenediamine adsorption takes place with one nitrogen down and the second nitrogen free, indicating that the propyl-sulfonic groups are separated beyond the span of accessibility to both nitrogens. Bonding of the conjugate bases in SBA is weaker than in Nafion-H, a fluorocarbon sulfonic acid, and sulfated zirconia (SZ). The N1s CLS of the SBA-bound nitrogen bases are substantially smaller than in Nafion-H and SZ and calculated adsorption energies are 55% smaller for pyridine bonded to propyl-sulfonic groups than to perfluoropropyl-sulfonic moieties. An all-electron theory accounts for the chemical CLS of both the S2p levels in the hydrogen-donor $-SO_3H$ and the N1s levels of the conjugate bases. The theory is validated by a linear correlation with experimental CLS of a polymer database presented in the Supporting Information section. A detailed analysis referring to specific results of section 4 is given below.

5.1. Pure SBA-15. The presence of a single S2p peak in the experimental spectrum (Figure 1) indicates one oxidation state of sulfur, and its BE of 169.25 eV confirms that it is the sulfur of the propylsulfonic acid group generated by a complete oxidation of the precursor mercaptopropyl groups. The peak width of 2.63 eV suggests a degree of heterogeneity among the sulfonic acid groups. The C/S ratio of 2.9 is close to the theoretical 3.0 predicted for the $-(CH_2)_3SO_3H$ species. This ratio demonstrates that all the excess Pluronic 123 was removed in the ethanol reflux, as a higher ratio would be observed otherwise.

Two theoretical models were employed. The "single site" model includes one $-SO_3H$ and one $-SH$ group, with the S2p levels separated by 5.27 eV (Table 3), in excellent agreement with the experimental difference of 5.15 eV found previously in a partially oxidized SBA material.[2] The second, "dual site" model involves two $-SO_3H$ groups in a sufficient proximity to interact. The $-SO_3H$ groups have only slightly different theoretical S2p energies in the single and the dual sites (to within ±0.1 eV, cf. Table 3 and Figure 6), however, even though the latter are tied together by weak hydrogen bonds (Figure 4). The S2p levels are therefore an adequate reference for CLS upon nitrogen base adsorption discussed in section 5.2 below.

5.2. Sorption of Nitrogen Bases. Adsorption of *pyridine*, a weak base, is widely used for the diagnostics of strong acid sites. In the case of Brønsted acid functionalities, interaction with pyridine may range from weak hydrogen bonding to a complete proton transfer to form a pair between the pyridinium cation and conjugate anion. The N1s XPS core levels in pyridine reflect this type of bonding by shifts to higher BEs, up to 3.6 eV (from the N1s BE of gaseous pyridine) in case of strong acids.[8] Simultaneously, atoms in the proton donor groups undergo CLS in the opposite direction to lower BEs. This was documented for the $-SO_3H$ functionalities in Nafion-H and the $-OSO_3H$ acid groups in SZ in our earlier work.[8] Even though adsorption of pyridine on the presently studied SBA-15 material was incomplete, with N/S ratio of 0.4 (Table 1), the CLS of the pyridine N1s of 2.35 eV (from the N1s BE of the "free" nitrogen of En adsorbed on SBA-15) to higher BEs and the S2p CLS of 0.80 eV (from the S2p of the bare SBA) to lower BEs observed (cf. Table 1) are consistent with the previous results[8] for pyridine adsorption on sulfur-based Brønsted acid sites.

Theoretical results for the KS orbital energies, where more negative theoretical orbital energies correspond to higher experimental BEs, fully support this trend, yielding N1s CLS on the order of −1.5 to −1.8 eV. We note that the free nitrogen of ethylenediamine has theoretical N1s level close to that of ammonia, cf. Table 3, cols. 3 and 5, rows 20−22. The calculated N1s of free pyridine is by 0.56 eV lower, cf. Table 3, and that of the polymers P4VP and P2VP with pendant pyridine groups

TABLE 4: Adsorption Energies of Pyridine, E_{ads}, and Theoretical N1S, S2s, and S2p Core-Level Shifts in Molecular Adducts of Pyridine with Ethylsulfonic Acid and Perfluoroethylsulfonic Acid (All Energies in eV, except E_{ads} in kJ/mol)

molecule or adduct[a]	total DFT energy	E_{ads}, kJ/mol	N1s orbital energy	S2s orbital energy	S2p orbital energy[b]	ΔN1s[c]	ΔS2s	ΔS2p
pyridine	−6755.87		-381.03			0.00		
$EtSO_3H$	−19146.05			−213.73	−159.87			
$Et(F_5)SO_3H$	−32648.74			−214.77	−160.90			
Py-$EtSO_3H$	−25902.44	−50.6	−382.23	−212.76	−158.90	−1.20	0.97[d]	0.97[d]
Py-$Et(F_5)SO_3H$	−39405.43	−78.7	−383.88	−212.92	−159.06	−2.84	1.85[e]	1.84[e]

[a] $EtSO_3H$, ethylsulfonic acid; $Et(F_5)SO_3H$, perfluoroethylsulfonic acid; Py-$EtSO_3H$, complex shown in Figure 7a; Py-$Et(F_5)SO_3H$, complex shown in Figure 7b. [b] Average of $S2p_x$, $S2p_y$, and $S2p_z$. [c] N1s core-level shift from free pyridine. [d] Core-level shift from $EtSO_3H$. [e] Core-level shift from $Et(F_5)SO_3H$.

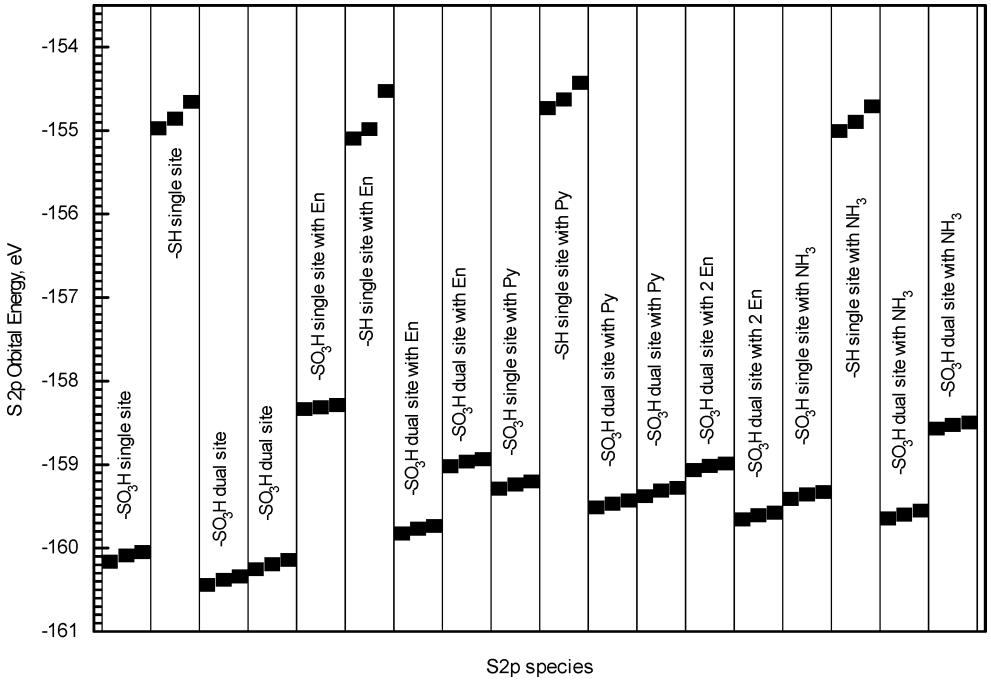

Figure 6. S2p orbital energies (DFT/BP/DN**) in the single and dual sites, their complexes with nitrogen bases. Each sulfur atom-containing species has three S2p levels associated with the $2p_x$, $2p_y$, and $2p_z$ orbitals.

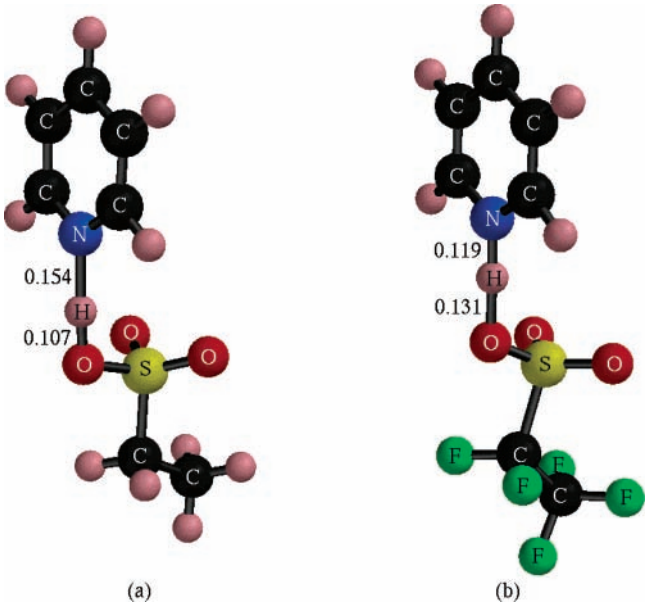

Figure 7. Pyridine complexes with (a) ethyl-sulfonic acid and (b) perfluoroethyl-sulfonic acid showing differences in the proton transfer from the $-SO_3H$ functionality to the nitrogen atom of pyridine due to substitution of aliphatic hydrogen by fluorine in the ethyl group. Calculations at the DFT/BP/DN** level with fully optimized geometries. The O−H and N−H distances are in nm.

by 0.3 eV lower, cf. Table S2 of Supporting Information. These theoretical results indicate that the N1s reference levels are uncertain to within 0.3−0.6 eV. However, the observed N1s CLS exceed this value and are accounted by the theory within this error margin. The S2p CLS are in the opposite direction of +0.8 eV to +0.9 eV for the two models (cf. Table 3), indicating again that the $-SO_3H$ groups are adsorption centers. The optimized geometry in Figure 5b confirms this but shows that proton transfer from the $-SO_3H$ groups to pyridine is far from complete. The calculated adsorption energies are −54.4 kJ/mol for single sites and −33.5 kJ/mol of pyridine for dual sites (Table 2), indicating a relatively weak acidity of the sulfonic acid functionalities in SBA-15 compared to Nafion-H, a fluorocarbon sulfonic acid. The pronounced effect of the fluorine substitution for hydrogen on the aliphatic chain carrying the $-SO_3H$ group is exemplified by the calculated sorption energies, structures and CLS of pyridine adducts with ethylsulfonic acid and perfluoroethylsulfonic acid (Table 4, Figure 7): adsorption energies are by 55% higher, the acidic proton is shifted by 0.3 Ångstrom toward the nitrogen atom, and N1s CLS is by 1.64 eV larger in the fluoro-derivative.

Ethylenediamine forms an adduct En-SBA which shows N1s CLS similar to Py-SBA to higher BEs for one of its two N atoms by 2.05 eV (from the "free" nitrogen of the adsorbed En), and S2p CLS to lower BEs by 1.10 eV from the S2p BE of the bare site (Table 1). The theoretical models yield the N1s CLS of −1.55 eV and −0.7 eV for the single and dual sites, and S2p CLS of +1.79 and +0.8 eV for the two sites. The theory thus supports single site adsorption of ethylenediamine with one nitrogen atom adsorbed and the second free, better than the dual site model. The optimized geometry in Figure 5c shows that proton transfer from the $-SO_3H$ groups to ethylenediamine is more pronounced than in the pyridine case. The calculated adsorption energy on single sites is −96.2 kJ/mol (cf. Table 2), consistent with stronger basicity of ethylenediamine than that of pyridine. The model with ethylenediamine bridging two $-SO_3H$ groups (Table 2, column 5) is discarded because the N1s CLS of the two bonded N atoms would be much smaller than observed.

The *ammonium-exchanged* NH_4−SBA material has been prepared from aqueous solution of NH_4Cl rather than by adsorption of NH_3. The resulting dry form of the ammonium ion-exchanged material, $-SO_3NH_4$, is equivalent to adsorbed ammonia on the protonated sulfonic groups, $-SO_3H\cdots NH_3$. The quantitation of the XPS spectrum indicates an incomplete exchange wherein slightly less than 30% of the $-SO_3H$ protons were replaced by ammonium ions, based on the experimental N/S ratio 0.29 (Table 1). The S2p levels at 169.30 eV of the bare $-SO_3H$ site and the shoulder at 168.60 eV of the occupied $-SO_3NH_4$ site show a CLS of 0.7 eV, in an excellent agreement

with theory that yields the S2p CLS of 0.73 eV for the single-site $-SO_3H\cdots NH_3$ (Table 3, column 4, row 16).

The SBA-15 material has been previously shown to be a catalyst for dehydrocondensation of alcohols to ethers, in particular with a 2/1 molar ratio of methanol to isobutanol to the methylisobutyl ether (MIBE), in excess to dimethyl ether (DME) from methanol and to isobutene (IB) from isobutanol.[2] The rates over this material are in the midrange of polymeric and inorganic solid acids,[2,5,30] but the selectivity toward the unsymmetrical MIBE is high and comparable only to that over Nafion-H.[31] One beneficial feature of the inorganic SBA is the presence of large nonswelling pores, in contrast to Nafion with swelling pores of undefined size. The present results show that further improvements of the SBA material for acid-catalyzed reaction are possible, specifically by derivatizing the silica inner surfaces by fluorocarbon sulfonic pendant groups for increased acid strength, and increasing the surface concentration of the acid functionalities for reactions that require molecular proximity of dual sites, as indicated by the kinetic behavior.[2]

Conclusions

The mesoporous SBA-15 material affords chemical versatility due to large pores and flexible pendant proton-exchanging $-SO_3H$ functionalities. There are some differences among individual preparations in terms of pore size, concentration of ion exchanging sites, completeness of oxidation of the precursor thiol groups, and successful removal of the organic templating agent.[1,2,6] The control of these properties and design of synthetic strategy for specific applications requires a thorough characterization, which is augmented by XPS and theory.

The present study shows that all of the organic templating agent can be removed and that the sulfur moieties can be fully oxidized to accessible $\equiv Si-(CH_2)_3SO_3H$ groups which exchange their protons with ammonium ions and adsorb nitrogen bases as proton-donor Brønsted acids. The $-SO_3H$ sites, although their concentration is comparable to polymeric sulfonated polyelectrolytes, are sufficiently separated so as not to be abridged by a short bifunctional base such as ethylenediamine. XPS has identified the proton donors through the S2p core-level shifts to lower BEs and the proton acceptors through the N1s core-level shifts of the adsorbed base to higher BEs.

The theory of core level shifts based on calculations of orbital energies has proven to be in excellent agreement with experiment, and in addition affords energies and optimized geometries of sorption adducts, including that of partial hydrogen transfer between the surface acid and the adsorbed base. The theory also has a predictive value in that one can calculate models of structurally and chemically different pendant groups that enable the control of acid strength and reaction pathways catalyzed by this mesoporous material.

Acknowledgment. We gratefully acknowledge the support of this work by the U.S. Department of Energy (DE-FG02-01ER15181). We thank Dr. John B. Higgins of Air Products and Chemicals, Inc. for the XRD analyses and Dr. Alfred C. Miller for professional and technical assistance with the XPS analyses using the Scienta ESCA facility of Lehigh University.

Supporting Information Available: Table S1, showing nitrogen-containing polymers and molecular models for calculations of N1s core level chemical shifts; Table S2, showing experimental binding energies and theoretical core levels of nitrogen-containing polymers and corresponding molecular models (eV); and Figure S1, showing the correlation between the DFT N1s orbital energies and the experimental N1s BEs of nitrogen-containing polymers; identification of the models for polymer segments and data from Table S1. This material is available free of charge via the Internet at http://pubs.acs.org.

References and Notes

(1) Margolese, D.; Melero, J. A.; Christiansen, S. C.; Chmelka, B. F.; Stucky, G. D. *Chem. Mater.* **2000**, *12*, 2448.

(2) Shen, J. G. C.; Herman, R. G.; Klier, K. *J. Phys. Chem.* **2002**, *106*, 9975.

(3) Shen, J. G. C.; Kalantar, T. H.; Ma, Q.; Herman, R. G.; Klier, K. *J. Chem. Soc., Chem. Commun.* **2001**, 653.

(4) Klier, K.; Kwon, H.-H.; Herman, R. G.; Hunsicker, R. A.; Ma, Q.; Bollinger, S. J. *Stud. Surf. Sci. Catal.* **2000**, *130D*, 3447 (12th International Congress on Catalysis, 2000, Pt. D).

(5) Klier, K.; Sun, Q.; Feeley, O. C.; Johanson, M.; Herman, R. G. *Stud. Surf. Sci. Catal.* **1996**, *101A*, 601 (11th International Congress on Catalysis—40th Anniversary, 1996, Pt. A).

(6) Melero, J. A.; Stucky, G. D.; van Grieken, R.; Morales, G. *J. Mater. Chem.* **2002**, *12*, 1664.

(7) Shen, J. G. C.; Kalantar, T. H.; Herman, R. G.; Roberts, J. E.; Klier, K. *Chem. Mater.* **2001**, *13*, 4479.

(8) Johansson, M.; Klier, K. *Top. Catal.* **1997**, *4*, 99.

(9) Hunsicker, R. A.; Klier, K.; Gaffney, T. S.; Kirner, J. G. *Chem. Mater.* **2002**, *14*, 4807.

(10) Klier, K. et al., to be published.

(11) Gelius, U.; Wannberg, B.; Baltzer, P.; Fellner-Feldegg, H.; Carlsson, G.; Johansson, C.-G.; Larsson, J.; Münger, P.; Vegerfors, G. *J. Electron Spectrosc. Relat. Phenom.* **1990**, *52*, 747.

(12) Chaney, R. L.; Simmons, G. W. *R&D Mag.* **1990**, *83* (9), 1.

(13) (a) Briggs, D.; Seah, M. P. *Practical Surface Analysis by Auger and X-ray Photoelectron Spectroscopy*; Wiley: Chichester, 1983. (b) Beamson, G.; Briggs, D. *High-Resolution XPS of Organic Polymers: The Scienta ESCA300 Database*; Wiley: Chichester, 1992.

(14) Brunauer, S.; Emmet, P. H.; Teller, E. *J. Am. Chem. Soc.* **1938**, *60*, 309.

(15) SPARTAN, ver. 3.1, Wavefunction, Inc., Irvine, CA.

(16) Becke, A. D. *Phys. Rev. A* **1988**, *38*, 3098.

(17) Perdew, J. P. *Phys. Rev. B* **1986**, *33*, 8822.

(18) The DN** basis set uses polarization functions for hydrogen, is equivalent in performance to Gaussian 6-31G**, and its construction follows that in Delley, B. *J. Chem. Phys.* **1990**, *92* (1), 508 (Wavefunction, Inc., private communication).

(19) Ma, Q.; Klier, K.; Herman, R. G. *Proceedings of the 74th ACS Colloid and Surface Science Symposium*, Lehigh University, Bethlehem, PA, 2000; American Chemical Society: Washington, DC, 2000; Abstract p 196.

(20) Klier, K. *Top. Catal.* **2002**, *18*, 141.

(21) Klier, K., to be published.

(22) Methfessel, M.; Fiorentini, V.; Oppo, S. *Phys. Rev. B* **2000**, *61*, 5229.

(23) Zhao, D.; Feng, J.; Huo, Q.; Melosh, N.; Frederickson, G. H.; Chmelka, B. F.; Stucky, G. D. *Science* **1998**, *279*, 548.

(24) Luan, Z.; Hartmann, M.; Zhao, D.; Zhou, W.; Kevan, L. *Chem. Mater.* **1999**, *11*, 1621.

(25) Morey, M. S.; O'Brien, S.; Schwarz, S.; Stucky, G. D. *Chem. Mater.* **2000**, *12*, 898.

(26) Van Grieken, R.; Calleja, G.; Stucky, G. D.; Melero, J. A.; Garcia, R. A.; Iglesias, J. *Langmuir* **2003**, *19*, 3966.

(27) A theoretical investigation of a silica model slab with hexagonal unit cell containing three layers of SiO_2 with the silicon layer sandwiched by two layers of oxygen—resembling the (111) surface of β-cristobalite—was determined to have in-plane unit cell parameters $a = b = 0.53$ nm, with angle $\angle(a,b) = 120°$ (Ma, Q.; Klier, K.; Cheng, H.; Mitchell, J. W.; Hayes, K. S. *J. Phys. Chem. B* **2000**, *104*, 10618). With two silicon atoms per unit cell and a planar unit cell area of $(0.53\text{ nm})^2 \sin(120°) = 0.243\text{ nm}^2$, the silicon surface concentration is calculated to be 8.22 Si atom/nm^2.

(28) Nordberg, R.; Albridge, R. G.; Bergmark, T.; Ericson, U.; Hedman, J.; Nordling, C.; Siebahn, K.; Lindberg, B. J. *Ark. Kemi* **1968**, *28*, 257.

(29) Gasteiger, J.; Hutchings, M. J. *J. Chem. Soc., Perkin Trans.* **1984**, *2*, 559.

(30) Klier, K.; Beretta, A.; Sun, Q.; Feeley, O. C.; Herman, R. G. *Catal. Today* **1997**, *36*, 3.

(31) Nunan, J. G.; Klier, K.; Herman, R. G. *J. Catal.* **1993**, *139*, 406.